Porous Scaffolds from High Molecular Weight Polyesters Synthesized via Enzyme-Catalyzed Ring-Opening Polymerization

Rajiv K. Srivastava and Ann-Christine Albertsson*

Department of Fibre and Polymer Technology, School of Chemical Science and Engineering, KTH, Royal Institute of Technology, Stockholm, SE-100 44, Sweden

Received March 29, 2006; Revised Manuscript Received June 12, 2006

Several aliphatic polyesters have been synthesized until now using enzyme-catalyzed ring-opening polymerization (ROP) of different lactones, although their molecular weight, hence mechanical strength, was not sufficient enough to fabricate porous scaffolds from them. To achieve this target, 1,5-dioxepan-2-one (DXO) and ϵ-caprolactone (CL) were polymerized in bulk with Lipase CA as catalyst at 60 °C, and porous scaffolds were prepared from the polymers obtained thereof using a salt leaching technique. The CL/DXO molar feed ratio was varied from 1.5 to 10, and the reactivity ratios of CL and DXO were determined using the Kelen−Tudos method under such conditions of polymerization. NMR results showed a slightly lower CL/DXO molar ratio in the copolymers than in the feed due to high reactivity of DXO toward Lipase CA catalysis. The crystallinity of the PCL segment of the copolymers was affected by the presence of soft and amorphous DXO domains. The copolymers having high CL content were thermally more stable. The porosity of the scaffolds was in the range 82−88%, and the SEM analysis showed interconnected pores in the scaffolds. Of the two parameters which could affect the mechanical properties, viz., the copolymer composition and the scaffold pore size, the pore size showed a significant effect on the mechanical properties of the scaffolds. The porous scaffolds developed in this way for tissue engineering are free from toxic organometallic catalyst residues, and they are highly suitable for biomedical applications.

Introduction

An increasing demand for degradable aliphatic polyesters for tissue engineering has led to the extensive research in ring-opening polymerization (ROP) of lactones and lactides, yielding polyesters with various architectures and properties.[1,2] These polyesters have extensively been used in the form of three-dimensional porous scaffolds for cell growth studies and other tissue engineering applications.[3−5] Such applications require high-porosity scaffolds with interconnected pores to minimize the amount of implanted polymer and to increase the specific surface area for cell attachment and tissue in-growth. This facilitates uniform distribution of cells and allows the transport of nutrients and cellular waste products. Several techniques have been developed to construct porous polymer scaffolds, and out of those, particulate or salt leaching is the most versatile processing method where the porosity can be easily controlled by variation of the amount of leachable particles.[6,7] Moreover, the pore size of the porous structure can also be adjusted independent of the porosity by using particles of different sizes.

Poly(ϵ-caprolactone) (PCL) is one of the most widely studied aliphatic polyesters for such purposes due to its good biocompatibility, biodegradability, and permeability.[8−12] It has also been shown that many different cells show excellent cell attachment and growth on this polymer,[13,14] making it a well-suited material for tissue-engineering scaffolds. On the other hand, a limited range of mechanical properties was observed in PCL due to its semicrystalline nature (T_m = 60 °C and T_g = −65 °C), and it is also not possible to grind this polymer, not even under cryogenic conditions. Therefore, the methods to produce porous structures by combining compression molding of salt−polymer mixtures and salt-leaching are not suited for PCL. Completely amorphous polymers such as poly(1,5-dioxepan-2-one) (PDXO)[15] are thus useful for copolymerization to improve the properties of PCL. Our group has synthesized random and block copolymers of 1,5-dioxepan-2-one (DXO) and ϵ-caprolactone (CL) using different organometallic compounds, e.g., $Sn(Oct)_2$ and $Al(^iPr)_3$, as catalysts for the ROP.[16−21] Shalaby et al. have shown the isomorphic character of the copolymers of CL and DXO.[22]

Exponential growth has been observed in the past decade where enzymes were used as catalysts for ROP of lactones and lactides, and due to the enzyme's origin from natural sources, they have been taken as a substitute for the toxic, metal-based catalytic systems. Mild polymerization conditions, no toxicity, high enantio- and regioselectivity, and recyclability of enzymes give them an extra edge over the use of organometallic catalysts.[23−25] In our recent publication, we have shown the use of different alcohols as initiators for the ROP of CL and DXO using Lipase CA as catalyst.[26] With this approach, A−B−A-type block copolymers of CL and DXO were synthesized, where commercially available dihydroxyl-terminated PCL was used to initiate the ROP of DXO.

Although the enzyme-catalyzed polymerizations are environmentally highly advantageous, the large quantity of enzymes required for polymerization and formation of relatively low molecular weight polymers obstruct their employment in the industry. Due to this reason, this technique is still at the stage of infancy to generate polymeric materials which can be converted to any useful physical form. The aliphatic polyesters previously synthesized by us using enzyme catalysis were of high molecular weight when compared with other polyesters synthesized from enzyme catalysis;[26,27] however, the molecular

* Corresponding author. Prof. Ann-Christine Albertsson; Department of Fibre and Polymer Technology, Royal Institute of Technology, Teknikringen 56-58, 100 44 Stockholm − Sweden; Tel +46 8 790 8274; Fax +46 8 208477; E-Mail: aila@polymer.kth.se.

10.1021/bm060309w CCC: $33.50
Published on Web 07/22/2006

weight was not sufficient enough to fabricate porous scaffolds from them for tissue engineering. The objective of this article was to synthesize even higher molecular weight aliphatic polyesters than obtained before, by enzyme-catalyzed ROP, and to develop porous scaffolds, suitable as tissue implants, from them. For this purpose, CL and DXO were chosen to form random copolyesters due to their respective advantages as mentioned before. The polymerization setup was developed in such a way that high monomer conversion as well as high molecular weight of the polymer was obtained in a bulk polymerization system. The copolymers obtained thereof were fabricated in the form of three-dimensional porous scaffolds from polymer solution containing leachable particles, and the scaffold properties were evaluated by different techniques.

Experimental Section

Materials. Tetrahydro-4*H*-pyrane-4-one (Maybridge Chemical, U.K.), *m*-chloroperbenzoic acid (Acros, Belgium), dichloromethane, $MgSO_4$, $NaHSO_3$, $NaHCO_3$, NaCl, and diethyl ether (Labora, Sweden) were used as received. ϵ−Caprolactone (Aldrich, Germany) was dried and distilled over CaH_2 at reduced pressure prior to use. Novozyme 435 (activity approximately 10 000 PLU/g according to the supplier) was donated by Novozyme, Inc., Denmark. Novozyme 435 (Lipase-CA) is a lipase (B lipase) from *Candida antarctica* produced by submerged fermentation of a genetically modified *Aspergillus oryzae* microorganism absorbed on a microporous resin. It consists of bead-shaped particles with a diameter in the range 0.3−0.9 mm. The bulk density of Novozyme 435 is approximately 0.43 g/cm^3, and it has a moisture content of 1−2% w/w. DXO was synthesized in the laboratory.

Synthesis of 1,5-Dioxepan-2-one (DXO). The DXO was synthesized from tetrahydro-4*H*-pyran-4-one through Bayer-Villiger oxidation according to the method reported by Mathisen et al.[15] The DXO obtained was purified by recrystallization from diethyl ether and two subsequent distillations under reduced pressure. Finally, the monomer was dried over CaH_2 overnight and distilled under reduced pressure. ^{1}H NMR δ (ppm): 4.2 (t, 2H, -*CH*$_2$−OCO-), 3.8 (t, 2H, -*CH*$_2$−CH$_2$−OCO-), 3.7 (t, 2H, -*CH*$_2$−CH$_2$−COO-), 2.6 (t, 2H, -*CH*$_2$−COO-).

Synthesis of Copolymers. In a typical polymerization, the lactones (DXO and CL) and enzyme (5.0 wt % of the total monomers) were weighed in a round-bottom flask, having fittings for nitrogen purging, inside the glovebox. The flask was then immersed in an oil bath at 60 °C under continuous mechanical stirring for 12 h in nitrogen atmosphere. The flask was removed from the oil bath, and a sample of the crude reaction mixture was taken for ^{1}H NMR analysis to determine the percentage monomer conversion. The polymer was isolated by dissolving the reaction mixture in a small amount of chloroform, removal of enzyme by filtration, followed by precipitation in excess cold hexane. The polymer was dried under vacuum before analysis. Copolymers having different molar feed ratios of DXO and CL were synthesized in this way.

Scaffold Preparation. The copolymers were dissolved in $CHCl_3$ to form 5 wt % homogeneous solutions and were subsequently poured over NaCl (salt-grinded and meshed to have particle size less than 100 μm) in Petri dishes with a diameter of 9 cm. Each mixture was thoroughly blended using a glass rod and evenly distributed over the bottom of the Petri dish. The mixture was slowly air-dried for a week and then vacuum-dried for 2 days to ensure complete $CHCl_3$ evaporation. A two-step leaching process was then performed on the solidified mixture on the mold. The mold with scaffold was first immersed in methanol for about 20 min to wet and swell the scaffold and also to loosen it from the mold. The free scaffold was thereafter immersed in deionized water to dissolve the salt particles. The water was changed after every 20 min during the first hour and then once every hour for 5 h, followed by a water exchange 3−4 times every 24 h for 4 days. The scaffold was then dried to a constant weight in a vacuum oven.

Characterization. *NMR.* The monomer conversion and the copolymer composition were determined by ^{1}H NMR, and the monomer sequence in copolymers was evaluated using ^{13}C NMR spectroscopy. A Bruker Avance 400 MHz NMR instrument operating at 400.13 and 100.62 MHz for ^{1}H and ^{13}C, respectively, was used for this purpose. $CDCl_3$ was used as solvent as well as internal standard ($\delta = 7.26$ and $\delta = 77.0$ ppm).

SEC. The molecular weight of the polymers was determined by size exclusion chromatography (SEC) using dimethylformamide (DMF) as eluent at a flow rate of 1.0 mL/min. The injection volume was 50 μL. A Waters 717 plus auto-sampler and a Waters model M-6000A solvent pump equipped with a PL-EMD 960 light scattering evaporative detector, two PL gel 10 mm mixed B columns (300 × 7.5 mm) from Polymer Laboratories, and one Ultrahydrogel linear column (300 × 7.8 mm) from Waters, connected to an IBM-compatible PC were used. Narrow molecular weight polystyrene standards were used for calibration. Millenium version 3.20 software was used to process the data.

DSC. The thermal properties of the polymers were determined by differential scanning calorimetry (DSC) using a Mettler-Toledo DSC 820 module under a nitrogen atmosphere (nitrogen flow rate 80 mL/min) with a sample mass of 5 ± 1 mg and a heating rate of 5 °C/min. The samples were subjected to a heating−cooling−heating cycle from −70 to 100 °C, and the analysis was performed on the second heating plot.

The relative crystallinity of the PCL segment of different samples was calculated according to eq 1

$$w_c = \frac{\Delta H_f}{\Delta H_f^0} \times 100 \qquad (1)$$

where w_c is the crystallinity, ΔH_f is the heat of fusion of the sample, and ΔH_f^0 is the heat of fusion of 100% crystalline PCL. The value of ΔH_f^0 used for the calculations was 139.5 J/g.[28]

TGA. Thermal stability of the copolymers was evaluated by thermogravimetric analysis (TGA) using a Mettler-Toledo TGA/SDTA 851^e module under a nitrogen atmosphere (nitrogen flow rate 50 mL/min) with a sample mass of 10 ± 1 mg and a heating rate of 10 °C/min.

Tensile Testing. Tensile testing of the porous scaffolds was performed on an Instron 5566 equipped with pneumatic grips and controlled by a Dell 466/ME personal computer. The tensile measurements were made with a crosshead speed of 50 mm/min and an initial grip separation of 32 mm. The samples had dimensions of 80 × 5 mm^2 and a thickness of approximately 0.5 mm. The average thickness of each sample was calculated from five independent measurements with a Mitutoyo micrometer. The samples were preconditioned for 48 h at 50 ± 5% RH and 23 ± 1 °C. Five different samples from the same scaffold were tested in accordance with ASTM D882−95A.

SEM. Three sample pieces were randomly chosen from each porous scaffold. Pore size and surface characteristics were determined using JEOL JSM-5400 SEM at an acceleration voltage of 15 kV. The samples were mounted on metal studs and sputter-coated with gold−palladium (60%−40%) using a Denton Vacuum Desk II cold sputter etch unit operated at 45 mA for 3 × 15 s.

Porosity. The porosity (P) of the scaffolds was determined by measuring the dimensions and the mass of the scaffold using eq 2

$$P = \left[1 - \frac{d_p}{d}\right] \times 100 \qquad (2)$$

where $d_p = (m_p/V_p)$ is the scaffold density, and d is the density of a nonporous film fabricated using the same technique as used for the scaffold fabrication.

DMTA. Dynamic mechanical properties of the scaffolds were determined using TA Instruments DMTA Q800. The measurements were made in the tensile mode with a distance of 12.86 mm between the grips. The temperature for measurement was programmed from

Table 1. Random Copolymers of CL and DXO Synthesized by Lipase CA Catalyzed ROP in Bulk at 60 °C

	feed composition				polymer composition[b]			block length[c]			
polymer	CL	DXO	molar ratio	yield[a] (%)	CL	DXO	molar ratio	CL	DXO	M_n[d]	PDI[d]
1	60.4	39.6	1.5	67	56.7	43.3	1.3	2.25	1.74	105 000	1.1
2	74.7	25.3	3.0	71	72.3	27.7	2.6	3.52	1.36	90 200	1.2
3	79.1	20.9	4.0	73	75.8	24.2	3.1	4.14	1.30	60 000	1.8
4	83.2	16.8	5.0	81	82.2	17.8	4.6	5.55	1.18	60 000	1.4
5	87.4	12.6	7.0	81	85.1	14.9	5.7	7.32	1.16	44 000	1.5
6	90.9	9.1	10.0	82	89.1	10.9	8.1	9.30	1.12	43 000	1.8
7	100	0		67	100	0				31 000	1.7

[a] Determined by gravimetric analysis. [b] Determined by ^{1}H NMR of precipitated polymer. [c] Determined by ^{13}C NMR. [d] Determined by SEC using polystyrene standards.

−80 to 40 °C at a rate of 3 °C/min. The measurements were performed at 1 Hz, and a static force of 1 N was applied. The width of the samples was 5 mm, and the average sample thickness, as determined from five independent measurements using a Mitutoyo micrometer, was 0.1 mm.

Results and Discussion

The most advantageous feature of enzyme-catalyzed polymerizations is their environmentally friendly characteristics, besides mild reaction conditions and control of polymer architecture. On the other hand, the use of enzymes has its own disadvantages such as high cost, large quantity of enzymes required for polymerization, and formation of low molecular weight products.[25] Our main emphasis was to synthesize aliphatic polyesters via enzyme catalysis and to use them in biomedical applications because of their hydrolytic degradation to nontoxic hydroxyl−carboxylic acids which can be metabolized within the human body. Aliphatic polyesters synthesized by enzyme catalysis until now have not been shown to form porous scaffolds for biomedical applications, mainly due to the low molecular weight of the polymers which is not sufficient enough to show any mechanical strength. Biomedical applications such as tissue implants and artificial cartilage and skin require strong, elastic, and tough polymers which can withstand the specific requirements of these uses.

We have previously shown the homopolymerization of DXO and CL using Lipase CA as catalyst and also the use of pentene-2-ol, dihydroxyl-terminated PCL, and poly(ethylene glycol) (PEG) as initiators for Lipase CA catalyzed ROP of DXO and CL.[26,27] Terminal functionalized and triblock polyesters synthesized using different alcohols as initiators showed a number average molecular weight (M_n) in the range 3000−10 000 g/mol as determined by ^{1}H NMR (6000−23 000 g/mol when determined from SEC using polystyrene standards). Such an approach showed the use of alcohols as initiators to generate different architectures, although the porous scaffolds fabricated from those polymers collapsed, as the mechanical strength of the polymers was not high enough to withstand the requirement of porous structure. In this work, we synthesized random copolyesters of CL and DXO using Lipase CA as catalyst in a mechanically stirred reaction setup to achieve high monomer conversion as well as high polymer molecular weight. The copolyesters obtained thereof were fabricated in the form of porous scaffolds for tissue implant applications.

Lipase CA Catalyzed ROP of CL and DXO. Lipase CA (Novozyme 435) has a high polymerization activity for lactones, it can be easily removed from the final product by filtration, and it does not release any toxic metallic residues. When it was used as a catalyst for ROP of a mixture of CL and DXO in bulk at 60 °C, the reaction system could be described as a suspension of enzyme beads in the monomer, and an increase in viscosity was observed with time. In our earlier publication, we have reported the bulk polymerization of DXO as well as CL using lipase CA as catalyst at 60 °C.[27] The DXO was found to be more reactive than CL under Lipase CA catalysis. The CL might have acted as a poor substrate for the lipase-catalyzed polymerization due to its weak binding at the enzyme's active surface. The rates of monomer conversion for DXO and CL were found to be 0.48%/min and 0.21%/min, respectively, during the initial 1 h of bulk polymerization with Lipase CA at 60 °C.[27] In this work, random copolymers of CL and DXO were synthesized using Lipase CA as biocatalyst at 60 °C, as shown in Scheme 1.

Scheme 1. Polymerization of CL and DXO with Lipase CA

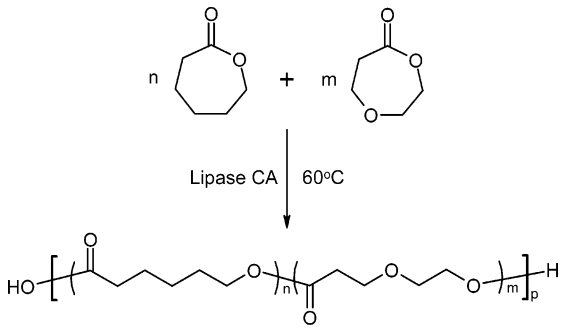

The molar feed ratio of monomers (CL/DXO) was varied from 1.5 to 10 as shown in Table 1. The monomer conversion was determined from ^{1}H NMR spectra of the crude reaction mixture by taking the ratio of peak intensities due to polymer and monomer. For DXO, the ratio of the intensities of oxymethylene protons of PDXO at 4.1 ppm (t, 2H, $-CH_2-$OCO−) and DXO at 4.2 ppm (t, 2H, $-CH_2-$OCO−) was used to calculate the percentage monomer conversion. In the case of CL, the ratio of peak intensities used to obtain the percentage monomer conversion was based on the oxymethylene protons at 4.0 ppm due to PCL (t, 2H, $-CH_2-$OCO−) and at 4.1 ppm due to CL (t, 2H, $-CH_2-$OCO−). The results showed more than 95% conversion for both monomers in all the polymerizations.

The polymer composition was calculated from the ^{1}H NMR spectra of precipitated polymer. The ratio of peak intensities due to PCL at 4.0 ppm and PDXO at 4.1 ppm was used for this purpose. A typical ^{1}H NMR spectrum of poly(CL-*co*-DXO) is shown in Figure 1. A slightly lower CL/DXO molar ratio was observed in the copolymers when compared with the CL/DXO feed ratio (Table 1). This was due to higher reactivity of DXO toward Lipase CA catalysis than CL. To prove the structure of the synthesized copolymers, sequence analysis was carried out in the carbonyl region of ^{13}C NMR spectra due to its greater sensitivity to sequence effects than ^{1}H NMR.[29] The ^{13}C NMR spectra of poly(CL-*co*-DXO) samples are shown in Figure 2.

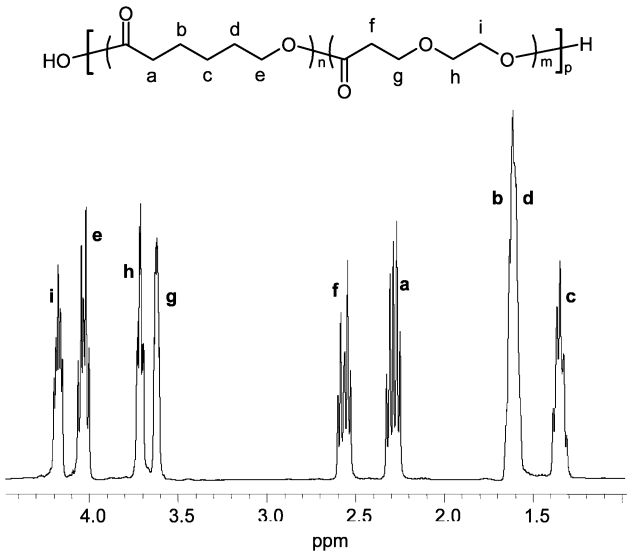

Figure 1. ^{1}H NMR spectrum of poly (CL-*co*-DXO) synthesized by Lipase CA catalyzed ROP of CL and DXO in bulk at 60 °C.

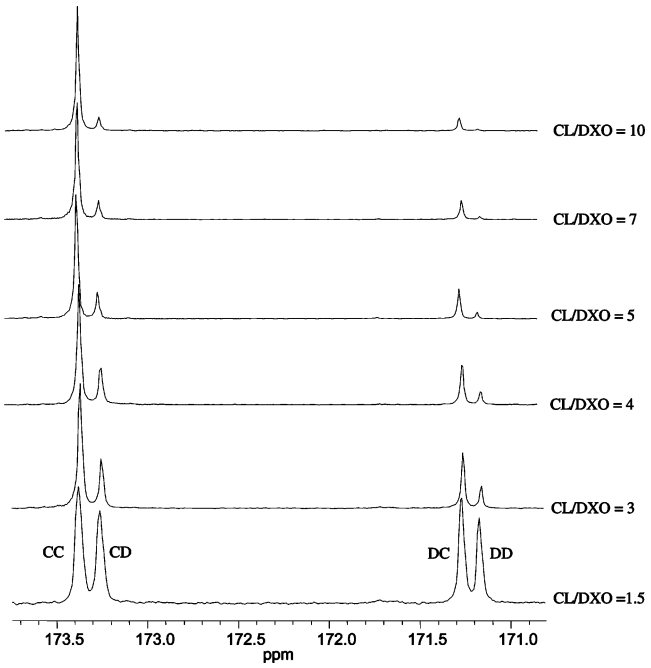

Figure 2. ^{13}C NMR spectra of poly(CL-*co*-DXO) synthesized by Lipase CA catalyzed ROP of CL and DXO; effect of CL/DXO molar feed ratio on the block length.

Four different peaks corresponding to the homopolymers and two dyads, i.e., transition between CL (C) and DXO (D), and vice-versa, are assigned in the spectrum. The spectra revealed the formation of a PCL block structure showing a high-intensity peak at 173.4 ppm due to the CL−CL (CC) sequence. The peak at 171.2 ppm due to the DXO−DXO (DD) sequence decreased as the CL/DXO molar ratio was increased. The average block lengths of PCL ($\bar{L}_{CL}$) and PDXO ($\bar{L}_{DXO}$) sequences were calculated from the intensities of carbonyl signals using eqs 3 and 4

$$\bar{L}_{CL} = \frac{I_{CC}}{I_{CD}} + 1 \tag{3}$$

$$\bar{L}_{DXO} = \frac{I_{DD}}{I_{DC}} + 1 \tag{4}$$

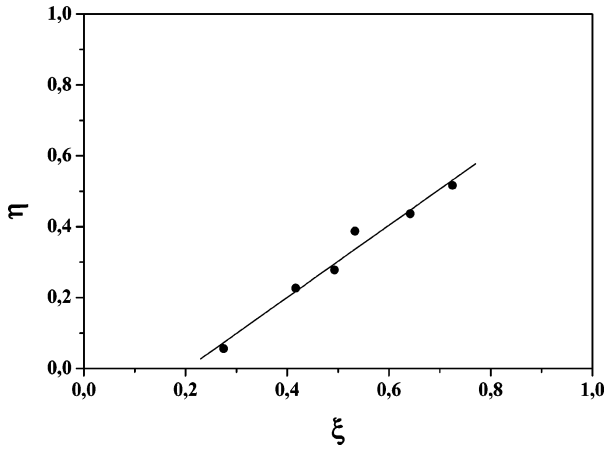

Figure 3. Reactivity ratio evaluation of the CL/DXO copolymer system using Kelen−Tudos method; r_{CL} = intercept at $\xi = 1$ and $-r_{DXO}/\alpha$ = intercept at $\xi = 0$, where α is a constant dependent on the conversion.

A respective increase in the PCL block length and decrease in the PDXO block length was observed as the CL/DXO molar feed ratio was increased from 1.5 to 10. The molecular weight of the copolymers was obtained from SEC, and the values of M_n and polydispersity index (PDI) are shown in Table 1. Higher DXO content in the feed resulted in high molecular weight copolymers due to its higher reactivity than that of CL. The PDI varied from 1.1 to 1.8 without showing any significant trend on the basis of copolymer composition. The high PDI values were a result of transesterification reactions, as both PDXO and PCL have a high probability of undergoing such reactions under these conditions of polymerization.

Reactivity Ratios. The reactivity ratios of CL and DXO under Lipase CA catalysis were determined using the method of Kelen and Tudos, which allows quite high conversions.[30] The composition of the reaction mixture was determined from ^{1}H NMR as described above. The reactivity ratios were calculated from a plot of eq 5

$$\eta = \left(r_1 + \frac{r_2}{\alpha}\right)\xi - \frac{r_2}{\alpha} \tag{5}$$

Figure 3 shows the resulting plot of Kelen−Tudos parameters η against ξ for the CL/DXO system, where r_1 and r_2 are determined from the intercepts, r_{CL} at $\xi = 1$ and r_{DXO} at $\xi = 0$, where α is a constant dependent on conversion. The plot gave the values $r_{CL} = 0.9$ and $r_{DXO} = 1.3$. These reactivity ratios showed that the obtained polymers are ideal copolymers, since $r_1 r_2 \approx 1$. As per the definition, the reactivity ratio is the ratio of self-propagation and cross-propagation, i.e.,

$$r_1 = \frac{k_{11}}{k_{12}} \quad r_2 = \frac{k_{22}}{k_{21}}$$

Substituting the experimentally determined reactivity ratios into these equations and rearranging gives the following relationships:

$$k_{12} = 1.1k_{11} \text{ and } k_{22} = 1.3k_{21}$$

Thus, in this copolymerization system, the DXO reacted 1.3 times faster than CL. In a previous study, when DXO and CL were homopolymerized under identical polymerization conditions, the rate of polymerization of DXO was found to be significantly higher than CL under Lipase CA catalysis.[27]

Table 2. Thermal Properties of Poly(CL-*co*-DXO)

polymer	T_m[a] (°C)	T_g[a] (°C)	W_c[a] (%)	T_g[b] (°C)
1	18.2	−52.9	52.1	−51.3
2	33.4	−56.2	54.4	−55.5
3	37.8	−58.4	59.7	−57.3
4	42.9	−59.8	60.1	−58.4
5	45.8	−61.2	63.1	−59.9
6	50.6	−62.1	69.3	−61.2
7	55.0	−64.5	72.4	

[a] Determined from DSC. [b] Calculated from FOX equation.

However, the reactivity ratio values of these two monomers were not much different in this study. This could be due to a "push mechanism" working when both the monomers were polymerized together. The higher reactivity of DXO rammed the reactivity of CL, which then became more recognizable by the enzyme in the presence of DXO. A similar trend in reactivity ratios, $r_{CL} = 0.6$ and $r_{DXO} = 1.6$, was observed in the literature when CL and DXO were polymerized using $Sn(Oct)_2$ as the catalyst.[17]

Thermal Properties. PCL is a semicrystalline polymer having a $T_m \approx 60$ °C, whereas PDXO is an amorphous polymer having $T_g \approx 39$ °C. In poly(CL-*co*-DXO) copolymers, the PCL segment showed a tendency to crystallize as revealed by the presence of a melting peak in the DSC thermograms. The crystallinity of the PCL segments was affected by the presence of the DXO units. The T_m decreased with an increase in DXO content because of the shortening of PCL crystalline blocks resulting in the formation of smaller and more imperfect crystals with a lower T_m (Table 2). The relative crystallinity of the PCL segments was calculated from the heat of fusion (melting peak) of different copolymers in comparison to the heat of fusion of 100% crystalline PCL. The crystallinity of the PCL segment of the copolymers, given in Table 2, decreased as the DXO content increased in the copolymers because of the hindrance created by the amorphous PDXO domains to the crystallization of the PCL blocks. A single glass transition between the glass transition temperatures of corresponding homopolymers was observed for all the copolymers. The T_g increased linearly with increase in the DXO content, indicating a random structure of the copolymers. The T_g values determined from DSC analysis were compared with the values obtained from the FOX equation in Table 2.

The thermal stability of the copolymers was analyzed by TGA. PCL or poly(CL-*co*-DXO) having a CL/DXO molar feed ratio of 10 showed a single-step degradation in the temperature range 350−450 °C. As the DXO content in the copolymers was increased, a two-step degradation was observed where the polymer degradation occurred between 250 and 300 °C as well. The TGA thermograms of poly(CL-*co*-DXO) having CL/DXO molar feed ratios of 1.5 and 10 are presented in Figure 4 to show this trend. The percentage weight loss occurring in both the steps is shown as a function of CL/DXO molar feed ratio in Figure 5. Higher DXO content resulted in higher weight loss in the first step (250−300 °C), and this showed that the copolymers having high amounts of CL were thermally more stable.

Scaffolds. The particulate leaching technique was used to develop the scaffolds from these copolymers. Methanol was used to remove the scaffolds from the Petri dishes, as methanol wetted and slightly swelled the scaffolds without leaching the salt or damaging the porous structure.[21] The porosity of the scaffolds was in the range 82−88%, and the results are presented in Table 3. The copolymers having a CL/DXO molar feed ratio of 3 or less could not be fabricated into scaffolds, as the porous structure collapsed during washing with methanol and water. Similar results have been observed before where scaffolds containing higher amounts of DXO were not stable enough to be removed from the mold surface.[21] The loss of porous structure was also observed when polyesters synthesized by us using enzyme catalysis in previous studies[26,27] were fabricated into scaffolds using the salt leaching technique.

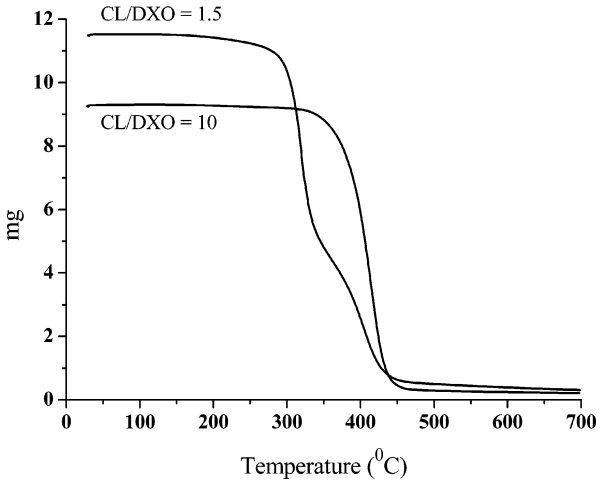

Figure 4. TGA thermograms of poly(CL-*co*-DXO) depicting change in the degradation profile when the CL/DXO molar feed ratio was changed from 1.5 to 10.

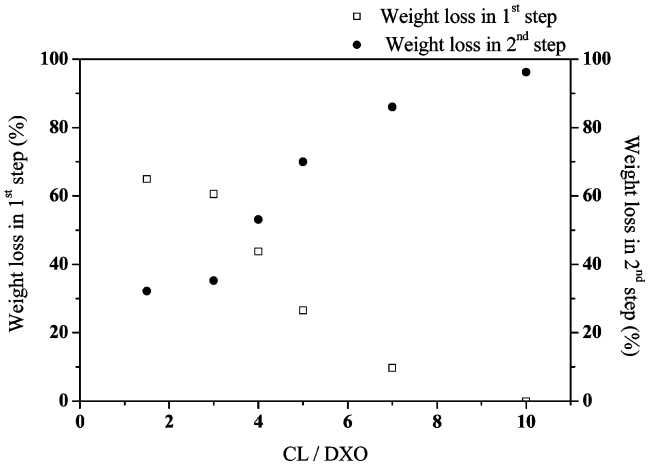

Figure 5. Effect of CL/DXO molar feed composition on the percentage weight loss in two steps as observed from the TGA thermograms.

Table 3. Properties of Poly(CL-*co*-DXO) Based Porous Scaffolds

polymer	scaffold stability	porosity (%)	avg pore size (μm)
1	not stable		
2	not stable		
3	stable	87.0	61
4	stable	88.3	48
5	stable	83.2	34
6	stable	82.0	40
7	stable	86.7	53

SEM. The shape, size, and interconnectivity of porous scaffolds developed using the particulate leaching technique govern the cell seeding and cell culture behavior. The SEM analysis of porous scaffolds of poly(CL-*co*-DXO) showed interconnected pores, so that the cells can grow throughout the scaffolds. The SEM pictures of poly(CL-*co*-DXO)-based scaffolds are shown in Figure 6. As shown in the SEM pictures, the scaffolds featured regular structures with homogeneously

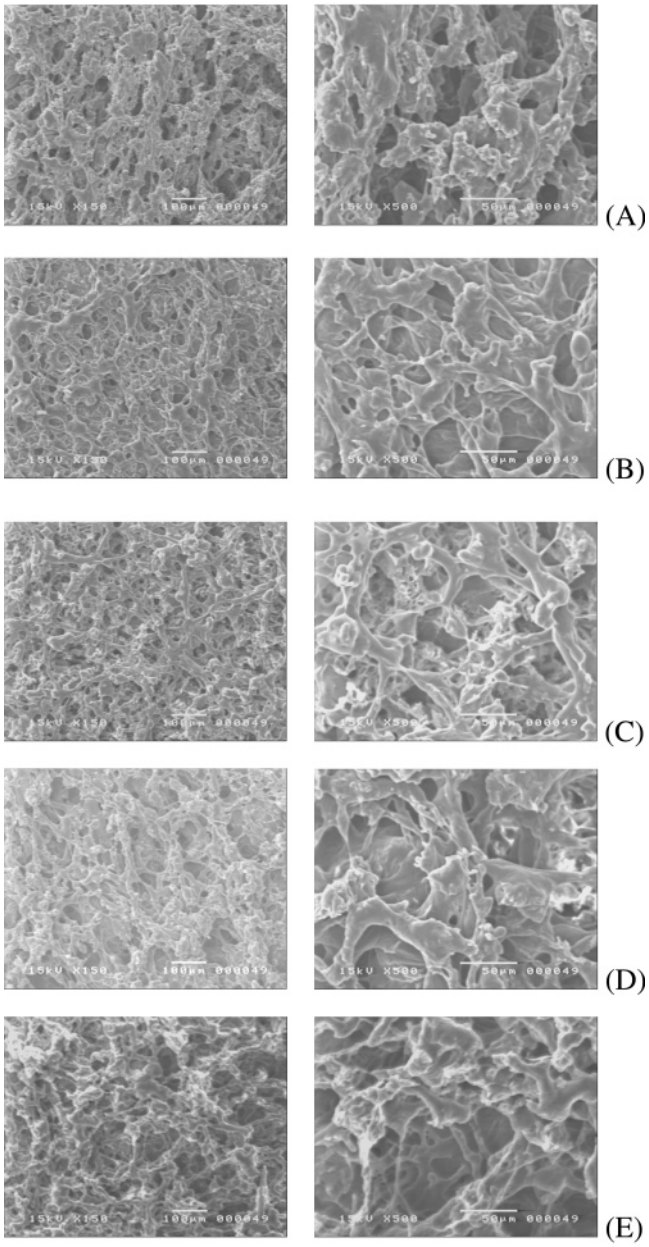

Figure 6. SEM micrographs of poly(CL-*co*-DXO) having different CL/DXO molar feed ratios (A) CL/DXO = 4, (B) CL/DXO = 5, (C) CL/DXO = 7, (D) CL/DXO = 10, and (E) PCL.

distributed pores. The surface topography of the porous scaffolds showed equivalent porosities and interconnectivities. The average size and size distribution of the pores was determined using image analysis, in which the pore diameter was plotted against their occurrence. The pore size was found to be less than 100 μm for all the scaffolds, although the average pore size and size distribution was slightly different for different scaffolds. The results are presented in Table 3 along with porosity values. Poly(CL-*co*-DXO) having CL/DXO molar feed ratio of 7 was found to have the smallest pore size, while that with a CL/DXO ratio of 4 had the largest pore size. This showed that the pore size was independent of the copolymer composition and totally depended on the size of salt particles used.

Tensile. The mechanical properties of poly(CL-*co*-DXO)-based porous scaffolds were expected to depend on two parameters: the copolymer composition and the pore size. The copolymers showed a single glass transition temperature in the DSC thermograms, indicating one amorphous phase and a crystalline domain of PCL segments. These soft−amorphous and hard−crystalline parts intertwined through chain segments incorporated in both domains can introduce thermoplastic elastomeric behavior. The tensile properties were thus expected to depend on the copolymer composition. The results from tensile testing are shown in Table 4. The scaffolds showed modulus values ranging from ~10 to 50 MPa, while the elongation at break varied from ~5% to 30%. Block copolymers of DXO and CL were synthesized before by our group, and nonporous films of those materials showed modulus values from 120 to 220 MPa and elongation at break of 900−1300%.[19,20] On the other hand, the tensile properties of these poly(CL-*co*-DXO)-based scaffolds showed similar values when compared with the porous scaffolds of CL and DXO synthesized using $Sn(Oct)_2$[21] (Table 4). No trend in tensile properties was observed if the copolymer composition was considered as a factor. On the other hand, it was deduced from the findings that the pore size had a significant effect on the tensile properties. The scaffolds developed from poly(CL-*co*-DXO) having a CL/DXO feed ratio of 7 showed the highest Young's modulus value. The scaffold from the same polymer had the smallest average pore size value (Table 3). The smaller the pore size of the scaffold, the more compact the porous structure would be, which in turn resulted into higher modulus. Correspondingly, the scaffold prepared by a CL/DXO feed ratio of 4 had the largest average pore size and relatively less continuous interconnections (Figure 6A) and as a consequence the lowest Young's modulus value. Thus, in this case, the tensile properties are affected by the pore size and structure of the scaffold rather than the copolymer composition. In addition to porosity aspects, it was also deduced from the results that a composition of 10−15% DXO gave an ideal balance between the strength and elasticity of the scaffolds.

Table 4. Tensile Properties of Poly(CL-*co*-DXO) Based Porous Scaffolds

polymer	modulus (MPa)	elongation at break (%)
3	10.0 ± 2.2	15.3 ± 2.5
4	20.5 ± 1.5	6.6 ± 1.9
5	45.8 ± 5.7	7.9 ± 2.1
6	26.2 ± 4.1	22.9 ± 5.6
7	15.2 ± 3.1	18.5 ± 1.1
a	13.0 ± 2.2	15.0 ± 6.3

[a] Poly(CL-*co*-DXO) synthesized using $Sn(Oct)_2$ as catalyst.[21]

DMTA. The storage modulus E', loss modulus E'', and loss factor tan δ versus temperature curves for poly(CL-*co*-DXO)-based scaffolds measured at a frequency of 1 Hz using DMTA are shown in Figures 7, 8, and 9, respectively. The scaffolds showed a sharp drop in the storage modulus in the temperature region corresponding to the glass transition, which confirmed the results from DSC analysis. The storage modulus was found to be higher for the samples containing lower amount of DXO (Figure 7). The loss modulus peak value decreased with increase in DXO content in the poly(CL-*co*-DXO)-based scaffolds, although no trend in the temperature value at loss modulus peak was observed (Figure 8). All samples exhibited a single sharp tan δ peak (Figure 9). The tan δ value was highest for the sample having the highest content of DXO. This indicated a greater relaxation strength due to a larger fraction of less-constrained chains participating in the relaxation. High DXO content gave more mobile chain segments, which consequently increased the relaxation strength. This became possible when high DXO content gave a large fraction of chain segments which were less constrained by PCL crystallinity. The high tan δ value for polymers **6** and **7**, containing relatively low amounts of DXO,

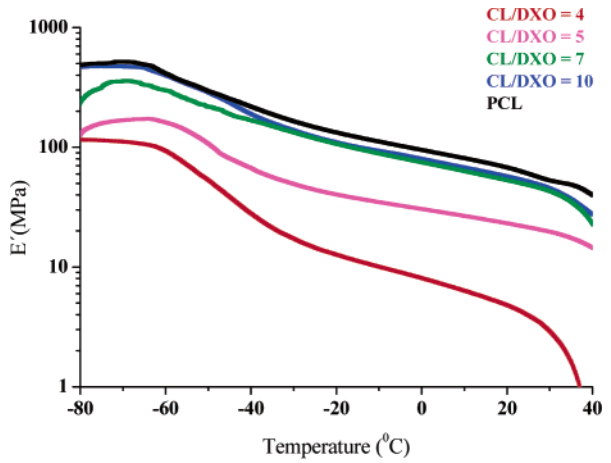

Figure 7. Storage modulus *E′* vs temperature for different poly(CL-*co*-DXO) copolymers measured using DMTA.

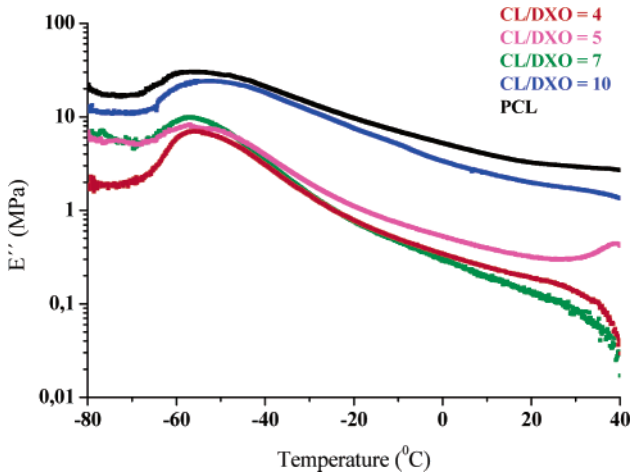

Figure 8. Loss modulus *E″* vs temperature for different poly(CL-*co*-DXO) copolymers measured using DMTA.

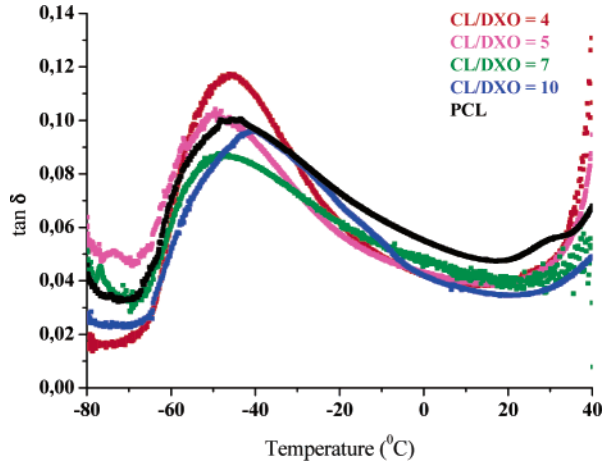

Figure 9. Loss factor (tan δ) vs temperature for different poly(CL-*co*-DXO) copolymers measured using DMTA.

could only be explained as a result of variation in pore size of the scaffolds. The temperature value at the tan δ peak showed no trend if polymer composition was considered as a factor. The values for loss modulus and tan δ are also presented in Table 5. The irregularities in peak temperature values of loss modulus as well as tan δ could again be explained due to the porous structure of the test samples, where the pores affected the DMTA results in the same way as the tensile properties discussed above.

Table 5. Results from DMTA Measurements of Poly(CL-*co*-DXO) Based Scaffolds

polymer	loss modulus peak (°C)	loss modulus (MPa)	loss tangent peak (°C)	loss tangent
3	−56.2	7.0	−45.7	0.117
4	−57.3	8.2	−49.6	0.102
5	−57.0	9.9	−48.0	0.087
6	−51.3	24.1	−40.5	0.096
7	−56.8	30.3	−45.3	0.100

Conclusions

High molecular weight random copolymers of CL and DXO synthesized via Lipase CA catalyzed ROP were effectively fabricated into porous scaffold structures using a particulate leaching technique. The polymerizations were performed to high monomer conversions in bulk at 60 °C using a mechanically stirred reaction setup. The reactivity ratios of CL and DXO determined using the Kelen−Tudos method showed values of $r_{CL} = 0.9$ and $r_{DXO} = 1.3$ under such conditions of polymerization. The CL/DXO molar ratio was slightly higher than that used in the feed due to higher reactivity of DXO than that of CL toward Lipase CA catalysis. The crystallinity of the PCL segments decreased as the amount of amorphous DXO domains increased in the copolymers. The copolymers containing higher CL content were thermally more stable. The scaffolds were highly porous, containing interconnected pores as revealed by the SEM analysis. The tensile as well as viscoelastic properties of the scaffolds were significantly affected by the porous structure of the samples. These scaffolds developed using polyesters synthesized from enzyme catalysis are free from toxic metallic residues and therefore better candidates for biomedical applications.

Acknowledgment. The authors thank SSF (The Swedish Foundation for Strategic Research); STINT (The Swedish Foundation for International Cooperation in Research and Higher Education), and The Royal Institute of Technology for financial aid for this work and Dr. Anna Wistrand for her support.

References and Notes

(1) Vert, M. *Biomacromolecules* **2005**, *6*, 538−546.
(2) Albertsson, A.-C.; Varma, I. K. *Biomacromolecules* **2003**, *4*, 1466−1486.
(3) Gunatillake, P. A.; Adhikari, R. *Eur. Cells Mater.* **2003**, *5*, 1−16.
(4) Agrawal, C. M.; Ray, R. B. *J. Biomed. Mater. Res.* **2001**, *55*, 141−150.
(5) Sahoo, S. K.; Panda, A. K.; Labhasetwar, V. *Biomacromolecules* **2005**, *6*, 1132−1139.
(6) Gogolewski, S.; Pennings, A. J. *Colloid Polym. Sci.* **1983**, *261*, 477−484.
(7) Thomson, R. C.; Yaszemski, M. J.; Powers, J. M.; Mikos, A. G. *J. Biomater. Sci., Polym. Ed.* **1995**, *7*, 23−38.
(8) Hutmacher, D. W. *J. Biomater. Sci., Polym. Ed.* **2001**, *12*, 107−124.
(9) Gurav, N.; Downes, S. *J. Mater. Sci.: Mater. Med.* **1994**, *5*, 784−787.
(10) Vert, M.; Li, S. M.; Spenlehauer, G.; Guerin, P. *J. Mater. Sci.: Mater. Med.* **1992**, *3*, 432−446.
(11) Pitt, C. G.; Chasalow, F. I.; Hibionada, Y. M.; Klimas, D. M.; Schindler, A. *J. Appl. Polym. Sci.* **1981**, *26*, 3779−3787.
(12) Schindler, A.; Jeffcoat, R.; Kimmel, G. L.; Pitt, C. G.; Wall, M. E.; Zweidinger, R. *Contemp. Top. Polym. Sci.* **1977**, *2*, 251−289.
(13) Walsh, D.; Furuzono, T.; Tanaka, J. *Biomaterials* **2001**, *22*, 1205−1212.
(14) Rizzi, S. C.; Heath, D. J.; Coombes, A. G. A.; Bock, N.; Textor, M.; Downes, S. *J. Biomed. Mater. Res.* **2001**, *55*, 475−486.
(15) Mathisen, T.; Masus, K.; Albertsson, A. C. *Macromolecules* **1989**, *22*, 3842−3846.

(16) Loefgren, A.; Renstad, R.; Albertsson, A. C. *J. Appl. Polym. Sci.* **1995**, *55*, 1589−1600.
(17) Albertsson, A. C.; Gruvegaard, M. *Polymer* **1995**, *36*, 1009−1016.
(18) Gruvegard, M.; Lindberg, T.; Albertsson, A. C. *J. Macromol. Sci., Pure Appl. Chem.* **1998**, *A35*, 885−902.
(19) Ryner, M.; Albertsson, A.-C. *Macromol. Symp.* **2001**, *175*, 11−18.
(20) Andronova, N.; Finne, A.; Albertsson, A.-C. *J. Polym. Sci., Part A: Polym. Chem.* **2003**, *41*, 2412−2423.
(21) Odelius, K.; Plikk, P.; Albertsson, A.-C. *Biomacromolecules* **2005**, *6*, 2718−2725.
(22) Shalaby, S. W.; Kafrawy, A. *J. Polym. Sci., Part A: Polym. Chem.* **1989**, *27*, 4423−4426.
(23) Kobayashi, S.; Uyama, H.; Kimura, S. *Chem. Rev.* **2001**, *101*, 3793−3818.
(24) Gross, R. A.; Kumar, A.; Kalra, B. *Chem. Rev.* **2001**, *101*, 2097−2124.
(25) Varma, I. K.; Albertsson, A.-C.; Rajkhowa, R.; Srivastava, R. K. *Prog. Polym. Sci.* **2005**, *30*, 949−981.
(26) Srivastava, R. K.; Albertsson, A.-C. *Macromolecules* **2006**, *39*, 46−54.
(27) Srivastava, R. K.; Albertsson, A.-C. *J. Polym. Sci., Part A: Polym. Chem.* **2005**, *43*, 4206−4216.
(28) Crescenzi, V.; Manzini, G.; Calzolari, G.; Borri, C. *Eur. Polym. J.* **1972**, *8*, 449−463.
(29) Kricheldorf, H. R.; Jonte, J. M.; Berl, M. *Makromol. Chem., Suppl.* **1985**, *12*, 25−38.
(30) Tudos, F.; Kelen, T.; Foldes-Berezsnich, T.; Turcsanyi, B. *J. Macromol. Sci., Chem.* **1976**, *A10*, 1513−1540.

BM060309W